Implementing Innovative Ideas in Structural Engineering and Project Management
Edited by Saha, S., Zhang, Y., Yazdani, and S., Singh, A.

ISBN: 978-0-9960437-1-7

ENERGY DISSIPATION IN POST-TENSIONED SELF-CENTERING PRECAST CONCRETE CONNECTIONS WITH A FRICTION DEVICE

TAKEAKI KOSHIKAWA

Faculty of Engineering, Hokkaido University, Sapporo, Japan

This paper presents an analytical study on the energy dissipation capacity of unbonded post-tensioned self-centering precast concrete beam-column connections that have a friction device only below the beam or on the web. The energy dissipation capacity is quantified using an effective energy dissipation ratio. To quantitatively evaluate the influence of three design parameters on the energy dissipation capacity, nonlinear analyses were carried out using a section-analysis method to predict the relationship between the moment and the relative rotation at the beam-column interface under cyclic loading. The design parameters were the initial post-tensioning force in the unbonded post-tensioning tendon, the friction force, and the location of the friction device. The analysis results show that the effective energy dissipation ratios for connections whose friction devices are in the same location can be related to the ratio of the friction force to the initial post-tensioning force.

Keywords: Unbonded, Prestressed concrete, Beam-column connection, Nonlinear section analysis.

1 INTRODUCTION

Post-tensioned self-centering beam-column connections with friction devices for precast concrete moment-resisting frames have been developed and investigated in several previous studies. These connections have unbonded post-tensioning tendons and friction devices. The tendons produce self-centering connection behavior, whereas the friction devices provide supplemental energy dissipation by allowing opening and closing of gaps at the beam-column interface under cyclic loading. The resulting moment-rotation responses of the connections exhibit flag-shaped hysteresis. In early research, the friction devices were placed on both the top and bottom surfaces of beams (Morgen and Kurama 2004), which led to the possibility of interference with the floor slab. To avoid such interference, connections were developed that had a friction device only below the beam or on the web. These performed well under cyclic loading (Sugiura *et al.* 2011, Song *et al.* 2014), but the influence of the design parameters on their energy dissipation capacity has not yet been revealed.

This paper presents an analytical study of unbonded post-tensioned self-centering precast concrete beam-column connections having a friction device. We carry out nonlinear analyses using a section-analysis method, and investigate the influence of several design parameters on the energy dissipation capacity of the connections.

2 CONNECTION ENERGY DISSIPATION

The behavior of an unbonded post-tensioned precast concrete beam-column connection with a friction device under cyclic loading is dominated by the opening and closing of the gap at the beam-column interface. The friction device, placed at the beam-end, is connected to the beam and the column, and dissipates energy for the connection via its friction force-displacement response as the gap opens and closes. Since the friction force provided by the friction device contributes moment resistance to the connection, the location of the friction device affects the hysteretic behavior of the connection. As an example, Fig. 1 shows schematic moment-rotation relationships for connections with friction devices at different locations, where M is the moment in the beam at the beam-column interface and θ is the chord rotation of the beam. If the friction device is located on the beam web (on the beam centerline), the hysteretic behavior of the connection is symmetric as shown in Fig. 1(a). If the friction device is located below the beam, the connection has an asymmetric behavior with different moment and energy dissipation capacities under positive and negative loading, as shown in Fig. 1(b).

The energy dissipation capacity of the connections is quantified using the effective energy dissipation ratio β_E, defined as the ratio of the hysteresis loop area for the connection to the area of a bilinear elastic-plastic connection with the same capacity (Seo and Sause 2005). For a connection with asymmetric behavior, β_E is defined as the average of the effective energy dissipation ratios defined for positive and negative loading responses (Iyama *et al.* 2009). As shown in Fig. 1, the envelopes of the actual moment-rotation relationships of the connections are nearly bilinear. The stiffness reduction, however, occurs in a smooth and continuous manner. To calculate the value of β_E, the beginning of the stiffness reduction, termed the linear limit, needs to be estimated with respect to both positive and negative loading responses. Closed-form expressions for calculating the linear limit moments (denoted as M_{ll^+} and M_{ll^-} in Fig. 1), developed assuming stiffness reduction due to nonlinear behavior of concrete in compression at the beam end, are used in this paper.

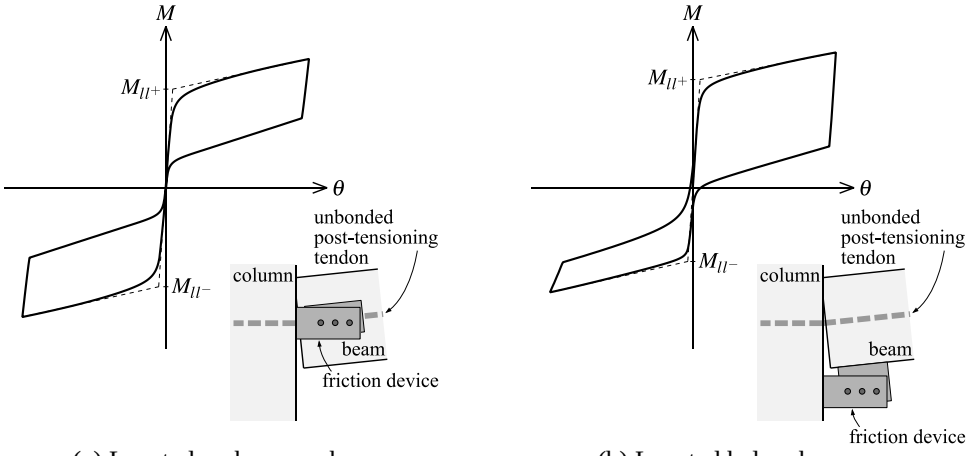

(a) Located on beam web. (b) Located below beam.

Figure 1. Moment-rotation relationships for connections with friction devices in different locations.

3 NONLINEAR SECTION ANALYSIS

This section describes a parametric analytical investigation of the energy dissipation capacity of unbonded post-tensioned precast concrete beam-column connections with a friction device. The parametric investigation is based on the analytical results obtained by using the nonlinear section analysis method developed by Koshikawa *et al.* (2012).

The section analysis method uses an incremental iterative approach to predict the moment-relative rotation hysteretic response at the beam-column interface of the connection, while satisfying section equilibrium conditions. In this method, the beam-end cross section at the beam-column interface is composed of a discrete number of concrete fibers, unbonded post-tensioning tendons, and friction devices. Each component in the cross section has a corresponding uniaxial constitutive relationship for each material: the stress-strain relationship for concrete in compression, the stress-strain relationship for post-tensioning tendons in tension, and the force-deformation relationship for the friction device. The axial deformations in each component are calculated as functions of the relative rotation and the relative axial displacement at the beam-column interface. The strains in the concrete fibers and the post-tensioning tendons are calculated by assuming that the strains are constant over the length of the concrete's compressive fracture zone and the unbonded length of the post-tensioning tendons. The stresses and the forces in each component are calculated from the uniaxial constitutive relationships. These calculations are iterated until the section equilibrium condition is satisfied by updating the value of the relative axial displacement. The moment corresponding to the relative rotation is derived once the equilibrium condition is satisfied, and the resulting forces and deformations in the beam-column subassemblages can be determined by considering the geometrical and mechanical properties.

Figure 2 shows the geometry, dimensions, material properties, and parameters for the unbonded post-tensioned precast concrete beam-column connection with a friction device used in the parametric investigation. Eighteen connections with different combinations of the design parameters were analyzed under cyclic loads applied at the tip of the beam. The main parameters that were varied were the initial post-tensioning

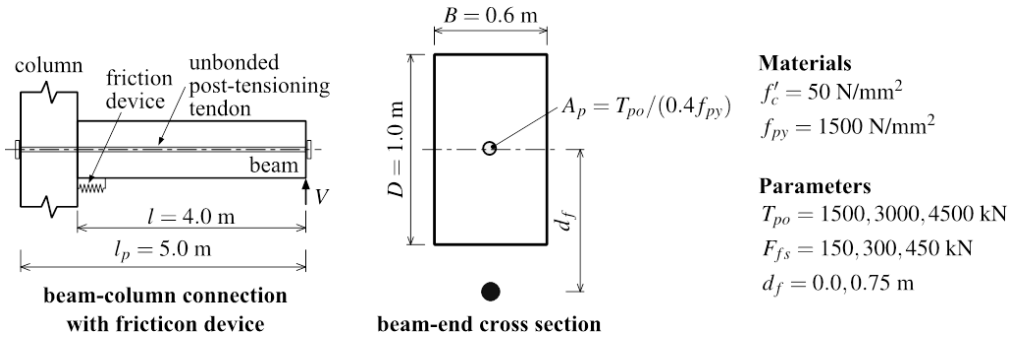

Figure 2. Unbonded post-tensioned precast concrete connection used in the parametric investigation.

force in the unbonded post-tensioning tendon T_{po}, the friction force F_{fs}, and the location of the friction device d_f. Three initial post-tensioning forces (T_{po} = 1500, 3000, and 4500 kN), three friction forces (F_{fs} = 150, 300, and 450 kN), and two friction device locations (d_f = 0.0, 0.75 m) were used. The values for T_{po} were set so that the initial compressive stresses in the beam concrete due to post-tensioning were equal to $0.05f_c'$, $0.10f_c'$, and $0.15f_c'$, respectively, where f_c' is the compressive strength of the beam concrete. The friction device locations d_f are the distances from the beam centerline of the connection. The value of d_f was set to 0.0 m for a friction device located on the beam web, and to 0.75 m for a friction device located below the beam.

For all of the connections, the initial stress of the unbonded post-tensioning tendon was 40% of the yield strength of the tendon f_{py}. The post-tensioning tendon area A_p was adjusted depending on the initial post-tensioning force T_{po}. The tendon was unbonded over the entire length l_p. We conducted the nonlinear section analyses of the connections while controlling the displacement, using the beam chord rotation θ as the control variable. The displacement history consisted of three cycles of sets of six rotations, having amplitudes of 0.005, 0.01, 0.015, 0.02, 0.025, and 0.03 rad.

The analytical moment-rotation ($M-\theta$) results for d_f = 0.0 m and 0.75 m for the connection having T_{po} = 3000 kN and F_{fs} = 300 kN are shown in Fig. 3. As mentioned earlier, the hysteretic behavior of the connection with d_f = 0.0 m is almost symmetric, while the behavior of the connection with d_f = 0.75 m is asymmetric. The moment and energy dissipation capacities of the connection in positive loading are larger than those in negative loading. The linear limit moments M_{ll^+} and M_{ll^-} shown in Fig. 3 are calculated using the following expressions:

$$M_{ll^+} = T_{po}\left(\frac{D-a_p-a_f}{2}\right) + F_{fs}\left(\frac{D-a_p-a_f}{2}+d_f\right) \tag{1}$$

$$M_{ll^-} = \begin{cases} -T_{po}\left(\frac{D-a_p-a_f}{2}\right) - F_{fs}\left(\frac{D-a_p-a_f}{2}-d_f\right) & \text{for } d_f = 0.0 \text{ m} \\ -T_{po}\left(\frac{D-a_p+a_f}{2}\right) + F_{fs}\left(\frac{D-a_p+a_f}{2}-d_f\right) & \text{for } d_f = 0.75 \text{ m} \end{cases} \tag{2}$$

where D is the beam depth. The terms a_p and a_f in Eqs. (1) and (2) are the components of the depth of the equivalent compression stress block contributed by the initial post-tensioning force and the friction force given by:

$$a_p = \frac{T_{po}}{0.85Bf_c'} \quad \text{and} \quad a_f = \frac{F_{fs}}{0.85Bf_c'} \tag{3}$$

where B is the beam width. For the negative linear limit moment M_{ll^-}, the directions of the friction force in the connections with d_f = 0.0 m and 0.75 m are different, and Eq. (2) provides two expressions for each case. These expressions estimate the linear limit moments reasonably well when compared to the analytical results.

Figs. 4 and 5 plot the effective energy dissipation ratio β_E against the friction force F_{fs} for the 18 connections, and the ratio of the friction force to the initial post-tensioning force F_{fs}/T_{po}, respectively.

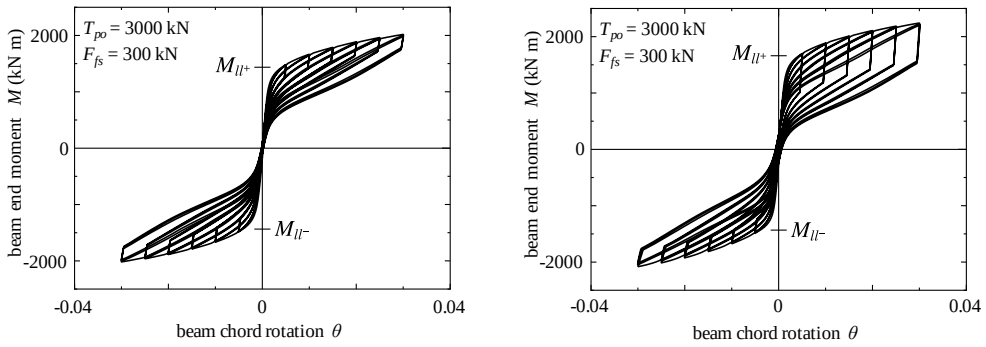

(a) d_f = 0.0 m (b) d_f = 0.75 m

Figure 3. Analytical moment-rotation response and calculated linear limit moment.

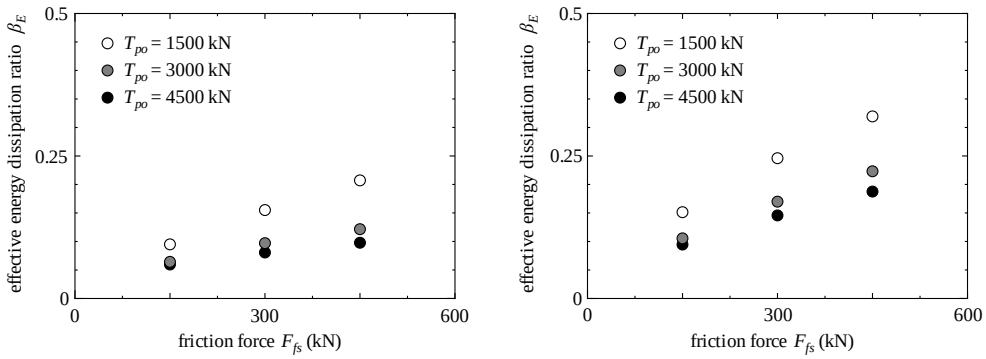

(a) d_f = 0.0 m (b) d_f = 0.75 m

Figure 4. Relationship between effective energy dissipation ratio and friction force.

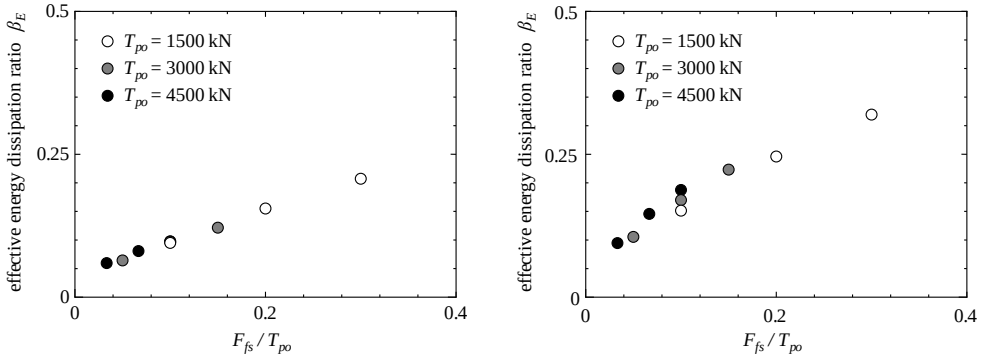

(a) d_f = 0.0 m (b) d_f = 0.75 m

Figure 5. Relationship between effective energy dissipation ratio and ratio of friction force to initial post-tensioning force.

Each value of β_E is calculated using the hysteresis loop area from the analytical results and the expressions for the linear limit moments, and is the average of the third cycles for all the rotation sets. As can be expected, increasing F_{fs} leads to an increase in β_E. Also, d_f affects β_E, since the moment lever arm between the friction force in the friction device and the concrete compressive stress resultant differs depending on the friction device location. For connections with the same friction forces and friction devices in the same locations, increasing T_{po} reduces β_E. This is because a higher initial post-tensioning force results in a larger positive linear limit moment $M_{ll}{}^{+}$ and a smaller negative linear limit moment $M_{ll}{}^{-}$, as shown in Eqs. (1) and (2), and does not significantly increase the hysteresis loop area. In addition, unlike the relationship between β_E and F_{fs} shown in Fig. 4, the relationship between β_E and F_{fs}/T_{po} is nearly proportional for each d_f shown in Fig. 5.

4 SUMMARY AND CONCLUSIONS

We analytically investigated the energy dissipation capacity of unbonded post-tensioned precast concrete beam-column connections with a friction device, using a nonlinear section analysis method to evaluate the influence of design parameters on the effective energy dissipation ratios. Three design parameters considered were the initial post-tensioning force in the unbonded post-tensioning tendon, the friction force, and the location of the friction device. To calculate the effective energy dissipation ratio, closed-form expressions for the linear limit moments were presented. We used the results of the nonlinear section analysis for 18 connections with different combinations of design parameters. They indicated the effective energy dissipation ratio could be increased by increasing the friction force, decreasing the initial post-tensioning force, and increasing the moment lever arm between the friction force and the concrete compressive stress resultant related to the friction device location. They also indicated the effective energy dissipation ratio for connections having friction devices in the same location may be related to the ratio of friction force to initial post-tensioning force.

References

Iyama, J., Seo, C. Y., Ricles, J. M., and Sause, R., Self-centering MRFs with Bottom Flange Friction Devices under Earthquake Loading, *Journal of Constructional Steel Research*, 65(2), 314-325, 2009.

Koshikawa, T., Kadowaki, H., and Matsumora, M., Energy Dissipation Efficiency of Unbonded Post-Tensioned Precast Concrete Beam-Column Connections with Beam-End Dampers, *Proceedings of the 15th WCEE*, Paper No. 812, Lisbon, Portugal, 2012.

Morgen, B. G., and Kurama, Y. C., A Friction Damper for Post-tensioned Precast Concrete Moment Frames, *PCI Journal*, 49(4), 112-133, 2004.

Seo, C. Y., and Sause, R., Ductility Demands on Self-centering Systems under Earthquake Loading, *ACI Structural Journal*, 102(2), 275-285, 2005.

Song, L. L., Guo, T., and Chen, C., Experimental and Numerical Study of a Self-centering Prestressed Concrete Moment Resisting Frame Connection with Bolted Web Friction Devices, *Earthquake Engineering and Structural Dynamics*, 43(4), 529-545, 2014.

Sugiura, H., Sashima, Y., and Sanada, Y., Performance Evaluation Tests of Unbonded Prestressed Concrete Beams with/without a Friction Damper, *Proceedings of the 20th SDPC*, 107-112, Hakodate, Japan, 2011 (in Japanese).